Toxicology and Applied Pharmacology 334 (2017) 24–34

Contents lists available at ScienceDirect

Toxicology and Applied Pharmacology

journal homepage: www.elsevier.com/locate/taap

Comparative health effects in mice of Libby amphibole asbestos and a fibrous amphibole from Arizona

Jean C. Pfau[a,*], Brenda Buck[b], Rodney V. Metcalf[b], Zoie Kaupish[a], Caleb Stair[a], Maria Rodriguez[a], Deborah E. Keil[a]

[a] Department of Microbiology and Immunology, Montana State University, Bozeman, MT 59717, USA
[b] Department of Geoscience, University of Nevada Las Vegas, Las Vegas, NV 89154, USA

ARTICLE INFO

Keywords:
Amphibole
Asbestos
Autoantibodies
Lung fibrosis
Pleural fibrosis

ABSTRACT

This project developed from studies demonstrating that Libby Amphibole Asbestos (LAA) causes a non-typical set of health outcomes not generally reported for asbestos, including systemic autoimmunity and an unusual and devastating lamellar pleural thickening that progresses to severe pulmonary dysfunction and death. Further, mineral fiber mixtures with some similarities to LAA have recently been discovered in southern Nevada and northwestern Arizona, where the material exists in extensive recreational areas and is present in yards, roads, parking lots and school yards. The objective was to compare the health outcomes in mice exposed to either LAA or the fibrous amphiboles collected in Arizona at the Lake Mead National Recreational Area at very low doses to represent environmental exposures. In this study, the fibrous amphibole asbestos sample from Arizona (AzA) is composed of winchite (69%), actinolite (22%), and non-amphibole minerals (9%) and has a mean aspect ratio of 16.7 ± 0.9. Fibrous amphibole asbestos from Libby (LAA) is composed of winchite (70%), richterite (9%), tremolite (5%), and non-amphibole minerals (16%) with a mean aspect ratio of 8.4 ± 0.7. C57BL/6 mice were exposed by oropharyngeal aspiration to fiber suspensions at a very low dose of 3 μg/mouse. After seven months, both LAA- and AzA-exposed mice had indices of chronic immune dysfunction related to a T_H17 cytokine profile, with B cell activation, autoantibody production and proteinuria, suggesting kidney involvement. In addition, both exposures led to significant lung and pleural fibrosis. These data suggest that there is risk of pulmonary disease and autoimmune outcomes with environmental exposure to amphibole asbestos, and that this is not limited to Libby, Montana.

1. Introduction

Multiple studies have chronicled the devastating health outcomes that resulted from asbestos exposure in Libby, Montana. While the rates of pulmonary fibrosis (asbestosis) and cancer (mesothelioma, pulmonary carcinoma) are significantly elevated among people exposed to the Libby amphibole asbestos (LAA), the predominant negative health outcomes include systemic autoimmunity and a progressive pleural fibrosis that may also be autoimmune in nature through production of mesothelial cell autoantibodies (MCAA) (Peipins et al., 2003; Pfau et al., 2005; Rohs et al., 2008; Sullivan, 2007; Szeinuk et al., 2016; U.S. Environmental Protection Agency, R, 2011; Whitehouse et al., 2008; Winters et al., 2012; Larson et al., 2010a; Gilmer et al., 2016; Hanson et al., 2016; Marchand et al., 2012; Serve et al., 2013). Using a wildtype mouse model (C57BL/6), we have corroborated these outcomes in mice, providing a critical tool for evaluation of the relative toxicity of other mineral fibers (Blake et al., 2008; Ferro et al., 2013; Gilmer et al., 2015; Pfau et al., 2013; Pfau et al., 2008; Zebedeo et al., 2014).

LAA exposures occurred due to contamination of vermiculite, which was mined outside of Libby for decades and used throughout the community in buildings, gardens, and playgrounds. This meant that there was a wide range of exposures, from high occupational exposures to relatively low, environmental exposures (Noonan, 2006; Noonan et al., 2015). Recently, the Environmental Protection Agency (EPA) conducted a risk assessment specifically for LAA based on a study that showed that significant negative health effects were occurring at extremely low exposure levels (Lockey et al., 2015). LAA is the first asbestiform fiber for which a toxicity value (Reference concentration, RfC) has been derived to help define a remediation target that reduces to acceptable levels the risk of acquiring non-malignant respiratory

Abbreviations: ANA, antinuclear autoantibodies; AzA, Arizona amphibole asbestos; EDS, energy dispersive spectroscopy; EPMA, electron probe microanalysis; LAA, Libby amphibole asbestos; LERP, Libby Epidemiology Research Program; MCAA, Mesothelial Cell Autoantibodies; RfC, Reference Concentration; SAED, selected area electron diffraction

* Corresponding author at: Department of Microbiology and Immunology, 960 Technology Blvd, Rm120, Bozeman, MT 59718, USA.
E-mail addresses: jean.pfau@montana.edu (J.C. Pfau), buckb@unlv.nevada.edu (B. Buck), metcalfr@unlv.nevada.edu (R.V. Metcalf), Deborah.keil@montana.edu (D.E. Keil).

http://dx.doi.org/10.1016/j.taap.2017.08.022
Received 14 June 2017; Received in revised form 26 July 2017; Accepted 31 August 2017

disease. The RfC_{LAA} was released on December 8, 2014 at 0.00009 PCM f/cm^3 (Phase Contrast Microscopy fibers/cm^3) (U.S. Environmental Protection Agency, R, 2015). The dramatic outcome of this fiber-specific health assessment, based on a specific non-cancer outcome (pleural fibrosis), emphasizes the need to evaluate health impacts based on variable mineral fiber composition from different sites. Similar to the study used by the EPA, the Libby Epidemiology Research Program (LERP, ATSDR, TS000099-01) has shown that 50% or more of people exposed to Libby Amphibole suffer from pleural scarring, and that this scarring can dramatically impact pulmonary function, eventually leading to significant disability and death (Szeinuk et al., 2016; Black et al., 2014). Amphibole mineral fibers are found in soils and rock outcroppings in many parts of the U.S. and around the world, leading to human exposures to naturally occurring asbestos (NOA) through numerous routes, including land development, recreation, and use of the material in roads, parking lots, and playgrounds (Abakay et al., 2016; Bayram & Bakan, 2014; Carbone et al., 2016; Cooper et al., 1979; Environmental Protection Agency, US, 2008; Paoletti et al., 2000; Van Gosen, 2007; Wylie & Candela, 2015). Thus, the public health impacts of on-going, current exposures, in addition to exposures over the last few decades, could be tremendous. Land use decisions in areas where NOA fibers are discovered need to be based on strong data that can be used in evaluating the application of the very low Libby RfC more broadly to other amphibole NOA.

Amphibole asbestos (fibrous amphiboles) has been reported in rocks, soils, dust, and air from areas in southern Nevada and northwestern Arizona on either side of the Colorado River near Hoover Dam (Buck et al., 2013; Metcalf & Buck, 2015; Tetra Tech, I, 2014). The amphibole asbestos material exists in extensive recreational areas and is present in yards, roads, parking lots and school yards in and around Boulder City, Nevada (Buck et al., 2013; Metcalf & Buck, 2015). These materials continue to be disturbed both by road construction/urban development but also by natural desert processes that produce dust storms throughout the year. Human exposures may already be extensive. The pathogenicity of this material is unknown, although environmental exposure to asbestos in southern Nevada is supported by a study showing atypical distribution of mesothelioma among women and young people (Baumann et al., 2013; Baumann et al., 2015). Amphibole asbestos in southern Nevada is predominantly the regulated mineral actinolite, while on the Arizona side the dominant asbestos mineral, referred to here as Arizona amphibole asbestos (AzA), is winchite, and is similar in composition and morphology to LAA. The relative pathogenicity may determine the need for a public health risk assessment for both cancer and non-cancer outcomes in this region. This study was designed to initiate this critical area of study, using our well-characterized mouse model.

2. Materials and methods

2.1. Amphibole minerals

LAA was provided by the EPA as a composite sample of asbestos-rich rock samples collected from multiple sites in the W.R. Grace mine outside of Libby, Montana. The LAA sample was previously characterized using a suite of methods including transmission electron microscopy (TEM) with selected area electron diffraction (SAED) (Duncan et al., 2014); scanning electron microscopy (SEM) with energy dispersive spectroscopy (EDS) (Gavett et al., 2016), x-ray diffraction (Lowers et al., 2012), and wavelength dispersive electron probe microanalysis (EPMA) (Meeker et al., 2003).

The fibrous amphiboles in this Arizona-Nevada region originated by hydrothermal alteration of granitic host rocks where asbestos minerals were precipitated as fracture-fill veins. In order to produce an AzA sample of high purity, a single sample of AzA in a centimeter-wide, asbestos-rich vein was collected from granitic rock of the Wilson Ridge pluton in the Lake Mead Recreation Area in northwestern Arizona. We used dental tools to separate AzA fibers in the vein from the rock matrix. This method decreases the amount of contaminant accessory minerals such as quartz, feldspar, and mica, which co-occur with the fibrous amphiboles. Scanning electron microscope-energy dispersive spectroscopy (SEM-EDS) analyses were performed on 470 particles to measure particle size and shape, and mineral chemistry. Wavelength dispersive electron probe microanalysis of a polished thin section of the AzA vein material provided quantitative chemical analyses that were used to classify the AzA minerals, methods comparable to that used by the USGS to classify LAA samples (Meeker et al., 2003). Characteristics of these fibers are summarized in Table 1. The fibers used in the current study are shown in columns 1 and 3 of Table 1.

Table 1
Fiber characteristics.

Characteristics	LAA (whole sample)[a,b]	AzA (amphibole only)	AzA (whole sample)[b]
Mineralogy	Winchite (70%), Richterite (9%), Tremolite (5%) Non-Amphibole (16%)	Winchite (76%), Actinolite (24%)	Winchite (69%), Actinolite (22%), Non-Amphibole (9%)
Morphology			
Analytical method	TEM	SEM	SEM
Min width (μm)	0.05	0.2	0.2
Max width (μm)	3.0	17.5	45.6
Mean width (μm)	0.36 ± 0.01	0.7 ± 0.1	1.3 ± 0.2
Min length (μm)	0.2	1.0	1.0
Max length (μm)	43.6	151.0	151.0
Mean length (μm)	2.3 ± 0.2	9.0 ± 0.7	9.7 ± 0.7
Min aspect ratio	1.0	1.0	1.0
Max aspect ratio	145.3	263.4	263.4
Mean aspect ratio	8.4 ± 0.7	18.2 ± 1.1	16.7 ± 0.9
Number of particles	510	427	470

[a] Data from (Duncan et al., 2014; Lowers et al., 2012; Meeker et al., 2003).
[b] Used in the current study.

All fibers were suspended in sterile phosphate buffered saline (PBS, pH 7.4), and sonicated (Branson Ultrasonics, Danbury, CT) for 5 min prior to use to minimize aggregation of the fibers.

Endotoxin testing of the fiber suspensions was performed using the PyroGene® Recombinant Factor C Endotoxin Detection System (Cambrex Bioscience, Walkersville, MD), following the manufacturer's protocol. Tested samples included the sterile PBS, suspended LAA (1.0 and 0.1 mg/ml) in sterile PBS, suspended AzA (1.0 and 0.1 mg·ml) in sterile PBS, plus *E. coli* O111·B4 (Sigma, St Louis, MO) lipopolysaccharide (LPS)-spiked samples, all against a standard curve provided with the kit. Briefly, all prepared samples and standards were placed in a 96-well plate at 100 μl/well, and incubated for 10 min at 37 °C. Detection working reagent was prepared and then added to all wells, and the plate was read immediately on a fluorescence plate reader (Fluorskan Ascent FL, ThermoFisher) at 380 excitation/440 emission. The plate was incubated for an hour at 37 °C, then read again with the same settings using the Ascent Software, to allow calculation of the change in fluorescence (ΔRFU), which was then plotted against the standard curve. Endotoxin was not detected in any of the samples, with a detection limit of 0.01 EU/ml.

2.2. Mice and exposures

All experiments with mice were approved by the Montana State University Institutional Animal Care and Use Committee (IACUC). The mice used were wild type C57BL/6 (Charles River, Seattle, WA) maintained in the Montana State University Animal Resource Center. These mice were housed under specific pathogen free (SPF) conditions

with 12 h light-dark cycle, constant temperature (22 °C) and humidity (45%), and ad libitum food and water. Both male and female mice were used between 6 and 8 weeks of age. Baseline cheek bleeds were used to evaluate autoantibody status at the beginning of the study, and initially, no mice were positive for antinuclear autoantibodies (ANA, methods described below).

2.3. Oropharyngeal instillations

Sterile suspensions of the fibers were prepared at 0.1 mg/ml in sterile saline. Mice were briefly anesthetized with isoflurane until breathing was slow and regular, but the animals were non-responsive. The tongue was pulled gently out of the mouth and to the side, and 15 μl were injected into the oropharynx using a micropipette (1.5 μg/mouse). Successful instillation was indicated by a deep breath of inhalation, and recovery from anesthesia was monitored. This procedure was repeated 2 weeks later, for a total dose of 3 μg/mouse. This dose was chosen to be within the range of environmental concentrations recorded in Libby, MT, since the main concern for exposure to "naturally occurring asbestos" (NOA) in Nevada and Arizona would be environmental (not occupational). Environmental exposures tend to be sporadic, due to dust storms or recreational activity in areas with NOA, rather than regular, all day, work exposures. In previous mouse exposure studies, a dose of LAA was chosen to represent cumulative occupational exposures in humans; but for this new study, a dose for LAA and AzA was selected to represent an environmental exposure.

A second cheek bleed was performed 4 months after the second instillation. Animal weights were monitored weekly. Initially, 20 mice were to be instilled in each group, but mice were lost due to death during instillation or during the 7 months due to excessive barbering that required euthanasia, which is not unusual with this strain. Ending mouse numbers were 14 saline control, 9 LAA and 17 AzA exposed mice that survived to the end of the experiment. 1 week prior to the end of the experiment, urine was collected from each mouse and assessed for proteinuria using albumin test strips (Albustix, Bayer Corp., Elkhart, IN). At 7 months after the last instillation, the mice were then euthanized by CO_2 asphyxiation, using IACUC-approved methods.

2.4. Tissues harvested

After euthanization, blood was collected by cardiac puncture, allowed to clot at room temperature, and then centrifuged to collect serum. Serum was stored at − 20 °C until use. 5 ml of sterile PBS with 5% fetal bovine serum (FBS) were injected into the intact peritoneal cavity, gently agitated, and then removed using an 18-gauge needle. This peritoneal wash fluid was centrifuged, and the cells were prepared for flow cytometry. Also harvested were lungs, diaphragms, and spleens. Lungs were weighed and fixed in Histochoice (Amresco, Solon, OH), and the diaphragms were fixed in Histochoice lying flat in 12-well tissue culture plates. The spleens were weighed, and then minced and prepared as single cell suspensions as previously described (Ferro et al., 2013), including a brief wash in Red Blood Cell Lysis solution (eBioscience/ThermoFisher; Waltham, MA) to select for white blood cells. The splenocytes were counted using a *Z*-series Coulter Counter (Beckman Coulter, Brea, CA), and 1 million cells from each sample were placed in two separate tubes containing 100 μl PBS with 3% Bovine Serum Albumin as blocking agent. Sets of cells were stained with BD Biosciences (San Jose, CA) antibodies as follows:

B cells: CD19 (PE) or IgM (PerCP Cy5.5)

B1a B cells: IgM^{pos} (PerCP Cy5.5), $CD5^{pos}$ (APC), $CD23^{neg}$ (PE)

B suppressor cells: $CD19^{pos}$ (PE), $CD5^{pos}$ (APC), $CD1d^{pos}$ (FITC), $CD11b^{pos}$ (PerCP Cy5.5)

T regulatory cells: $CD3^{pos}$ (PerCP Cy 5.5), $CD4^{pos}$ (PE), $CD25^{pos}$ (FITC), Fox $P3^{pos}$ (APC)

2.5. Flow cytometry

Cells were stained for 30 min at 4 degrees C, and then washed with 1 ml ice cold PBS, twice. Staining was analyzed on a FACS Calibur flow cytometer using Cell Quest software (BD Biosciences). Isotype control antibodies (BD Biosciences) determined background staining, and < 1% of these controls was allowed in the M1 gate for percent positive. Monocytes and Lymphocytes were determined based on forward and side scatter, and then the major subsets within the lymphocyte gate were identified based on the antibodies listed above. Tight polygonal regions were used (instead of quadrants) to identify the ultimate subpopulations.

2.6. Th1/Th2/Th17 cytometric bead array (CBA)

The cytometric bead array (CBA) mouse Th1/Th2/Th17 cytokine kit (BD Biosciences) examines seven cytokines in a single sample using fluorescent beads that can be analyzed using flow cytometry. These cytokines include interleukin-2 (IL-2), IL-4, IL-6, IL-17, IL-10, interferon-γ (IFN-γ), and tumor necrosis factor-α (TNF-α), and are associated with one of the three T-helper cell profiles, Th1, Th2, and Th17. The cytokines belonging to the Th17 profile have been associated with autoimmune diseases (Afzali et al., 2007; Furuzawa-Carballeda et al., 2007). The CBA procedure was carried out according to the manufacturer's instructions. To prepare the top standard, all seven of the lyophilized standard spheres were added to a 15 ml conical tube. The spheres were dissolved in 2.0 ml of the kit's assay diluent and incubated at room temperature for at least 15 min. The top standard was serially diluted to create the standard curve. A negative standard was also used which only contained assay diluent.

Creating the mixture of capture beads was done by calculating the appropriate amount of each bead solution to use based on the number of samples for that particular experiment. All seven of the bead solutions were added to a single 5 ml centrifuge tube. Fifty microliters of the capture bead mixture were added to each 1.5 ml micro centrifuge assay tube. Another 50 μl of the standards and samples were added the appropriate assay tube. Fifty microliters of PE detection reagent from the kit were added to all the assay tubes and incubated in the dark for 2 h at room temperature. One milliliter of wash buffer from the kit was added to all the assay tubes and then centrifuged at 200 g for 5 min. The supernatant was carefully removed still leaving some fluid to ensure the pellet was not discarded. The pellet was resuspended in 300 μl of wash buffer. All samples were analyzed on the FACS Calibur flow cytometer for acquisition and analysis following instrument set-up using the provided instrument set-up bead sets.

2.7. Anti-nuclear antibody (ANA) assay

The serum samples from cardiac punctures were analyzed for antinuclear antibodies (ANA). The ANA test (ImmunoConcepts, Sacramento, CA) is a semi-quantitative analysis that uses indirect immunofluorescence to detect any auto-reactive antibodies in the serum. The assay kit was modified for the use of mouse serum.

The serum was diluted at a 1:80 ratio by adding 5.0 μl of serum in 395 μl of PBS. Twenty microliters of each diluted sample were added to their corresponding wells on the HEp-2000 substrate slide and incubated at room temperature for 30 min. The slides were washed with PBS being careful not to cross contaminate any samples. The slide was then submerged in a staining dish with PBS for 10 min with gentle rotation. The slide was carefully dried by blotting in between the wells.

The fluorescent antibody reagent was prepared by adding 2.0 μl of goat anti-mouse IgG antibody conjugated to AlexaFluor 488 (Invitrogen, Eugene, OR) to 1.0 ml of PBS. Twenty microliters of the antibody solution was added to each well and incubated in the dark at room temperature for 30 min. The slide was washed as above and a cover slip was applied by placing four to five drops of Fluorsave

(Calbiochem, La Jolla, CA) along the midline of the slide then setting the cover slip. The slides were viewed using the FITC (488 nm) filter on a Nikon Eclipse 80i fluorescence microscope, using the 20 × and 40 × objectives. Positive and negative controls were included on each slide, and slides were read by two trained, blinded, independent readers to determine whether the sample was positive for ANA and to record staining patterns.

2.8. Detection of mouse serum mesothelial cell autoantibodies (MCAA)

A cell-based ELISA was performed as previously described (Gilmer et al., 2015) to test for the binding of serum antibodies to mesothelial cells. Briefly, mouse primary mesothelial cells were seeded at confluency on 96 well plates, attached overnight and fixed in 1% paraformaldehyde. Following washing with PBS-Tween (0.05%), cells were blocked with 5% non-fat dry milk/PBS and then exposed to serum from each mouse diluted in 3% BSA/PBS (1:100). Following a 2-h incubation with serum, cells were washed and blocked a second time. The secondary antibody HRP-conjugated goat anti-mouse IgG (Invitrogen) was applied at a dilution of 1:1000 in 3% BSA/PBS and incubated for 1 h. Excess antibody was removed and plates developed using TMB reagent (Thermo Scientific) followed by 50 µl 1 M HCl. Plates were analyzed at 450 nm on a SpectrMax microtiter plate reader (Molecular Devices, Sunnyvale, CA). Correction for non-specific secondary antibody binding was performed on a plate-to-plate basis by subtracting the mean optical density (OD) for the secondary antibody-only control wells from the mean OD of each sample. Samples were determined to be MCAA-positive (MCAA +) if the corrected OD was at least three standard deviations above the mean OD for control (normal, untreated) mouse serum.

2.9. QuickZyme hydroxyproline assay (right lung and diaphragm collagen)

The amount of collagen in the right lung and diaphragm of mice was determined by QuickZyme Total Collagen Assay (QuickZyme Biosciences, Leiden, The Netherlands) according to the manufacturer's instructions. Right lungs were collected and weighed. Two same-sized (4 mm) tissue punches were obtained from the diaphragm of each mouse. The right lungs and the combined tissue punches from each mouse were hydrolyzed overnight in 0.5 ml or 100 µl (respectively) of 6 M HCl at 95 °C and then the hydroxyproline was oxidized. After staining the hydroxyproline residues with QuickZyme stain, absorbance was measured at 540 nm on a Spectra-Max microtiter plate reader.

2.10. Statistical analyses

All graphs are representative of at least two experiments. Overall statistical differences were assessed by one-way ANOVA using StatPlus with Bonferroni post hoc testing (StatPlus Software, Walnut CA). Two-tailed *t*-tests were used to assess differences between two means, using StatPlus. Statistical significance was defined as p values < 0.05. Except for percentages (frequency), data are graphed with error bars indicating standard error of the mean.

3. Results

3.1. Fiber mineralogy and morphology

Morphology and mineralogy of LAA and AzA are shown in Table 1. Both whole samples have similar mineralogy (Table 1, columns 1 and 3). The LAA sample is reported to be 84% amphiboles, with the remaining 16% composed of various minerals including feldspar, quartz, talc and calcite (Lowers et al., 2012). The AzA sample is composed of 91% amphiboles and 9% other accessory minerals including quartz and feldspar. Amphibole mineralogy is similar for both AzA and LAA samples: both are dominated by winchite (AzA 69%, LAA 70%) as determined by quantitative EPMA analyses (Meeker et al., 2003). Of just the AzA amphibole particles alone, 93% had aspect ratios 3.0 or greater, and the mean aspect ratio was 18.2 (± 1.1) (Table 1, column 2). Of the whole AzA sample with contaminant minerals included, 86% of the particles have aspect ratios 3.0 or greater, and the mean aspect ratio was 16.7 (± 0.9) (Table 1, column 3). The LAA sample overall has lower aspect ratios, with only 49% of particles having an aspect ratio 3.0 or greater. The mean width of the AzA particles was 1.3 (± 0.2) µm, which is essentially 3.6 times that of the LA, which was 0.36 (± 0.01) µm. This difference is artificial and reflects the different instrumentation used to characterize the fibers: the TEM is able to measure and identify significantly smaller particles than the SEM (Table 1). Although the AzA sample contains numerous tiny fibers, they were too small for the current instrumentation (SEM/EDS) to reliably measure and therefore those small particles were not included in the analyses. On-going analyses using field-emission scanning electron microscopy is planned in order to more fully characterize this sample.

3.2. Mouse health and weights

There was no significant difference in the average weights of combined male and female mice in each treatment group (data not shown, $p = 0.2$). As expected for this strain, male mice tended to be larger than females. The LAA-exposed females were slightly larger than saline females, but overall, weights did not change with treatment (Fig. 1). There were no obvious changes in health status over the 7 months in any group. Mice in all 3 groups lost fur particularly on their faces and necks, but without skin lesions. No tumors were found during tissue harvest.

3.3. Spleen weights and cell counts

There was no significant difference in the average spleen weights for the different treatments (Fig. 2, top). Although the splenocyte counts for LAA and AzA-treated mice were slightly higher than controls, these were not significant at an alpha level of 0.05 (Fig. 2, bottom). When corrected for body weight, AzA-treated female (but not male) mice showed increased numbers of splenocytes/g of mouse (Table 4).

3.4. Antinuclear autoantibodies (ANA) and mesothelial cell autoantibodies (MCAA)

At 4 months, LAA did not induce ANA above controls, but the

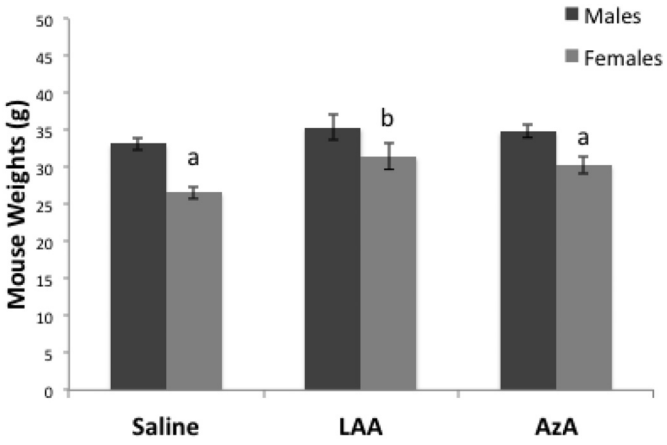

Fig. 1. Mouse weights at 7 months post-exposure. As expected, male mice tended to be larger than females. The LAA-exposed females were slightly larger than saline females. Saline: n = 14 (9 male, 5 female), LAA: n = 9 (4 male, 5 female), AzA: n = 17 (8 male, 9 female).
a = $p < 0.05$ compared with males in same treatment group; b = $p < 0.05$ compared to saline, same sex. Error bars = standard error of the mean (SEM).

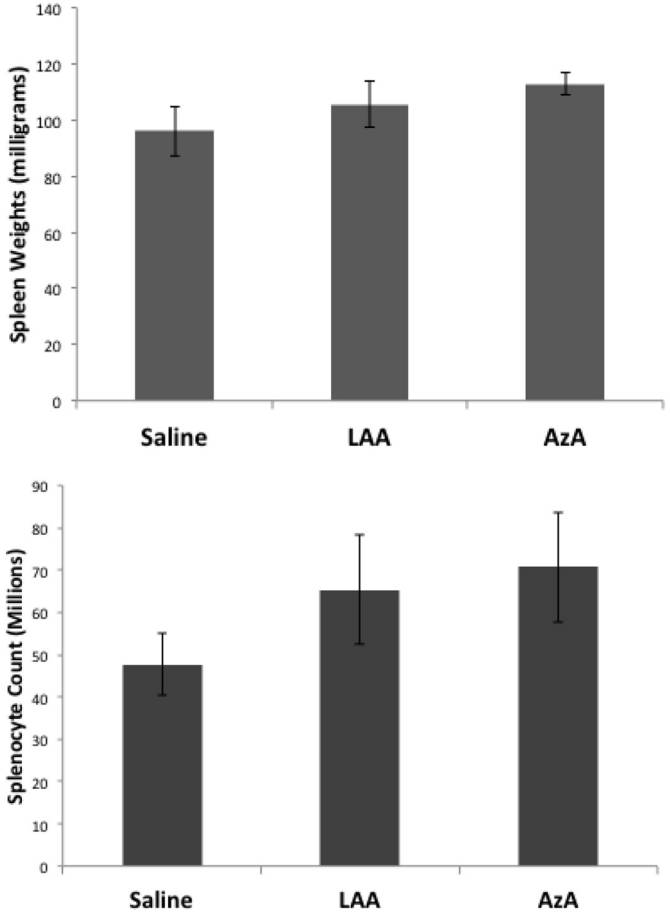

Fig. 2. Spleen weights (top) and cell counts (bottom). There were no significant differences in spleen weights or cell counts among the treatment groups. Saline: n = 14 (9 male, 5 female), LAA: n = 9 (4 male, 5 female), AzA: n = 17 (8 male, 9 female). Error bars = standard error of the mean (SEM).

percent positive for AzA was increased above saline controls (Fig. 3, top). By 7 months, both LAA and AzA had induced ANA, although LAA did not reach statistical significance at $p < 0.05$ ($p = 0.1$ by Fisher's Exact Test). Most of the positive ANA tests were from the female mice (Fig. 3, bottom).

MCAA were induced primarily by AzA at this dose, shown both by percent positive (Fig. 4, top) and MCAA score (a measure of binding absorbance) (Fig. 4, bottom). Again, most of the positive tests were in female mice (Table 5). Despite what appears to be increasing trends with dose in the percent positive and scores in both sexes, neither sex met statistical significance.

3.5. Urine albumin: proteinuria

Urine albumin was used as a measure of proteinuria, suggesting kidney involvement. Fig. 5 indicates that both LAA and AzA were affecting kidney function to a moderate degree, possibly by immune complex deposition (Pfau et al., 2008; Zebedeo et al., 2014). Positive tests were indicated by detection of albumin at > 30 mg/dL. There were no significant differences between males and females in any of the treatment groups (Table 4, Fisher's Exact Test).

3.6. Spleen lymphocyte subsets by flow cytometry

Lymphocyte subsets were evaluated by flow cytometry. Because the spleen weights and cell counts were not statistically different among the groups, much of the data is reported as percentage of the parent population. Fig. 6, top left, shows that while the numbers of T cells were

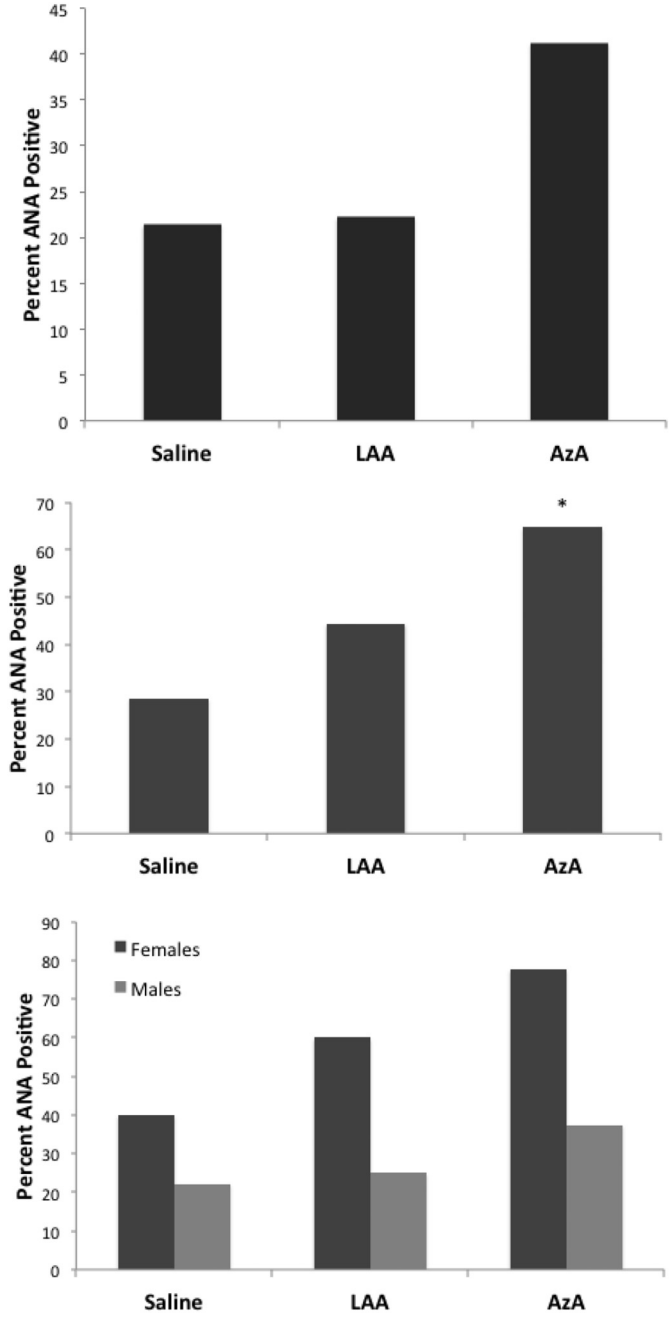

Fig. 3. ANA testing was done on commercial slides from ImmunoConcepts at 1:80 serum dilution. ANA were detected using anti-mouse IgG conjugated to HRP at a 1:1000 dilution. Top graph: ANA at 4 months post-exposure. Middle Graph: ANA at 7 months post-exposure. *Fisher's exact test gave a $p < 0.05$ for AzA compared to Saline controls. Bottom graph: most of the positive tests were from the female mice at 7 months. Mouse numbers were as in Fig. 1.

not significantly affected by treatment, both fiber types caused an increase in the number of B cells in the spleen. The increase in the number of splenic B cells for AzA was primarily in the female mice in this group, where the female mice had significantly more B cells/g mouse than males (Table 4). Table 4 also shows the percent positive of B cells and T cells separated by sex in each treatment group. With AzA, the percent of B cells increased, while the percent of T cells decreased in both sexes.

Fig. 6, top right, shows the T cell subsets of T helper cells (CD3 +, CD4 +) and T regulatory cells (CD4 +, CD25 +, FoxP3 +). The only significant difference was a reduction in the percentage of T regulatory cells with AzA treatment. There were no significant differences between the sexes for these subsets (data not shown).

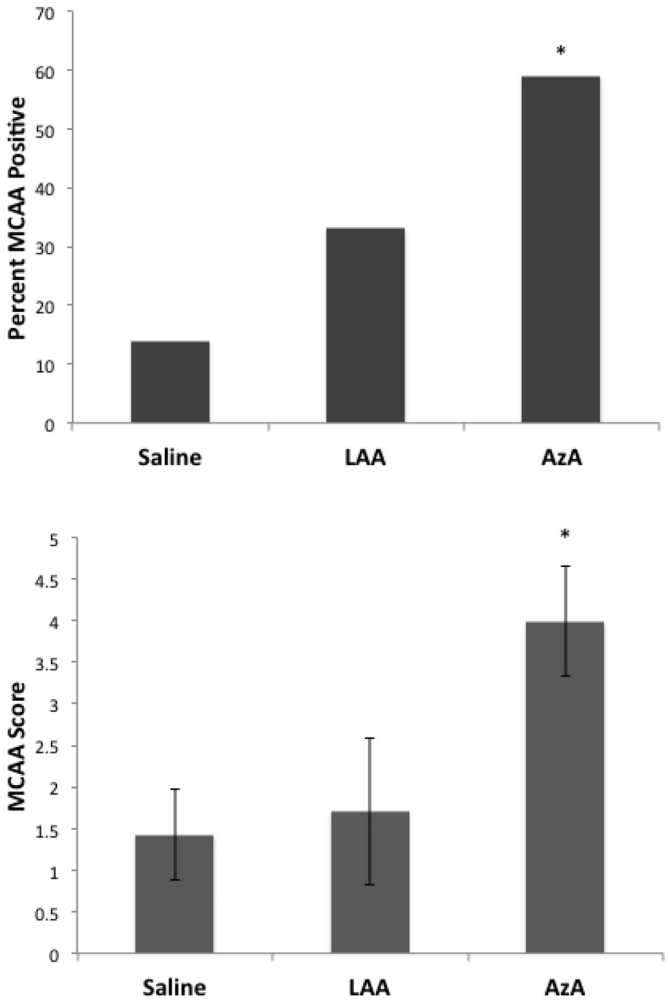

Fig. 4. MCAA measured by cell-based ELISA. Top graph: Percent positive for MCAA. * = $p < 0.05$ by Fisher's Exact Test. Bottom Graph: MCAA scores = number of standard deviations above the mean for the saline controls. Error bars = SEM. * = $p < 0.05$ compared to Saline controls and LAA. Mouse numbers were as in Fig. 1.

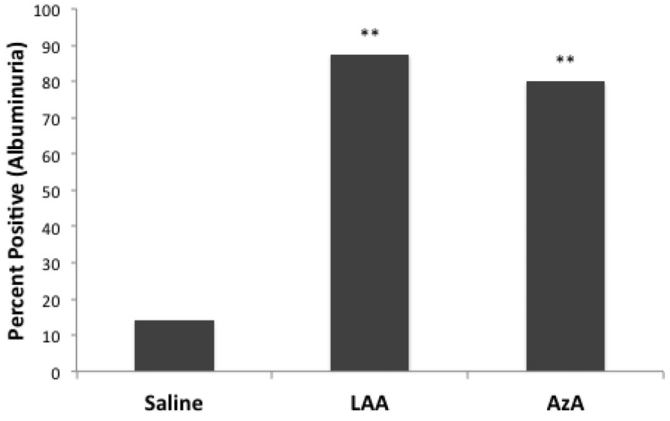

Fig. 5. Urine albumin was measured using Albustix with freshly collected mouse urine. The percent positive in each treatment group is graphed, where the positive/negative cut-off was 30 mg/dL; readings of "trace" albumin were considered negative. * = $p < 0.005$ by Fisher's Exact Test.
Mouse numbers were as in Fig. 1.

Fig. 6, bottom, shows the B cell subsets of B1a B cells (IgM +/CD5 +, CD23-) and suppressor B cells (IgM +, CD5 +, CD11b +, CD1 +). Both LAA and AzA led to a significantly greater percentage of B1a B cells among the lymphocyte population, with no significant difference in the mean percent positive for splenic suppressor B cells in any group. There were also no significant differences between the sexes for these subsets (data not shown).

3.7. Peritoneal lymphocyte subsets

Similarly, lymphocytes in the peritoneal wash fluid were evaluated by flow cytometry. There were no differences among the main populations found in the peritoneal cavity (monocytes and lymphocytes, Fig. 7, top), but among the lymphocytes there were moderate increases in B cells by both LAA and AzA (Fig. 7, bottom). However, consistent with previous studies (Pfau et al., 2013), the percent of lymphocytes that were B1a B cells was reduced with either LAA or AzA (Fig. 7, bottom). Interestingly, male mice contributed more to this effect than females (Table 2). Table 2 shows all of the subpopulation data for each treatment group for both sexes of mice. There was a decrease in the percentage of cells that would be considered suppressor B cells, particularly in the female mice. Overall, this meant that the ratio of B1a to suppressor B cells increased for females with fiber treatment, but decreased for males.

3.8. Serum cytokines by cytokine bead array (CBA)

Table 3 shows the CBA data for cytokines in the serum of the mice. The key finding was that both LAA and AzA triggered all three of the cytokines described as part of a T_H17 response: TNFα, IL-6, and IL-17. These T_H17 cytokines are shown in Fig. 8. Neither LAA or AzA triggered IL-2 or high levels of interferon gamma, which are essential for a T_H1 response. Further, neither fiber stimulated IL-4, which would have indicated a T_H2 response. There were a few differences between the sexes for LAA only, including IL-10, IFN gamma, and TNFα, where females tended to produce less of these cytokines (Table 3).

3.9. Lung and pleural collagen by hydroxyproline (QuickZyme) assay

Non-cancer pulmonary disease with LAA exposure includes a limited number of cases of interstitial fibrosis, with the predominant disease being pleural fibrosis (Peipins et al., 2003; Szeinuk et al., 2016; Black et al., 2014). In the mice, interstitial fibrosis was measured as total collagen in the right lung of each mouse. Fig. 9, top, demonstrates that excess lung collagen occurred with both LAA and AzA to a similar degree. Female mice had more lung collagen than males in controls, but this did not increase significantly with treatment (Table 5). Significant increases in lung collagen with fiber treatment occurred in the males. Pleural fibrosis was assessed as well, with the diaphragms assayed as parietal pleura. Fig. 9, bottom, shows the diaphragm collagen results, with excess collagen consistently occurring with both LAA and AzA. These increases occurred in both male and female mice, with no difference between males and females (Table 5).

4. Discussion

The revelation that the vermiculite mined for decades outside of Libby, MT, was contaminated with amphibole asbestos has led to multiple studies of the health outcomes of exposure to Libby Amphibole Asbestos (LAA). There remains no doubt that LAA can trigger mesothelioma, pulmonary carcinoma, interstitial fibrosis (asbestosis), and pleural fibrosis (Peipins et al., 2003; Rohs et al., 2008; Sullivan, 2007; Whitehouse et al., 2008; Winters et al., 2012; U.S. Environmental Protection Agency, R, 2015; Black et al., 2014; Antao et al., 2012; Bandli & Gunter, 2006; Benson et al., 2015; Dunning et al., 2012; Larson et al., 2010b; Larson et al., 2012a; Larson et al., 2012b; McDonald et al., 2004; Whitehouse, 2004), consistent with our general understanding of asbestos toxicity. However, its predominant health outcomes appear to be a progressive lamellar pleural thickening (LPT) (Szeinuk et al., 2016; Black et al., 2014), and systemic (rheumatic) autoimmune diseases

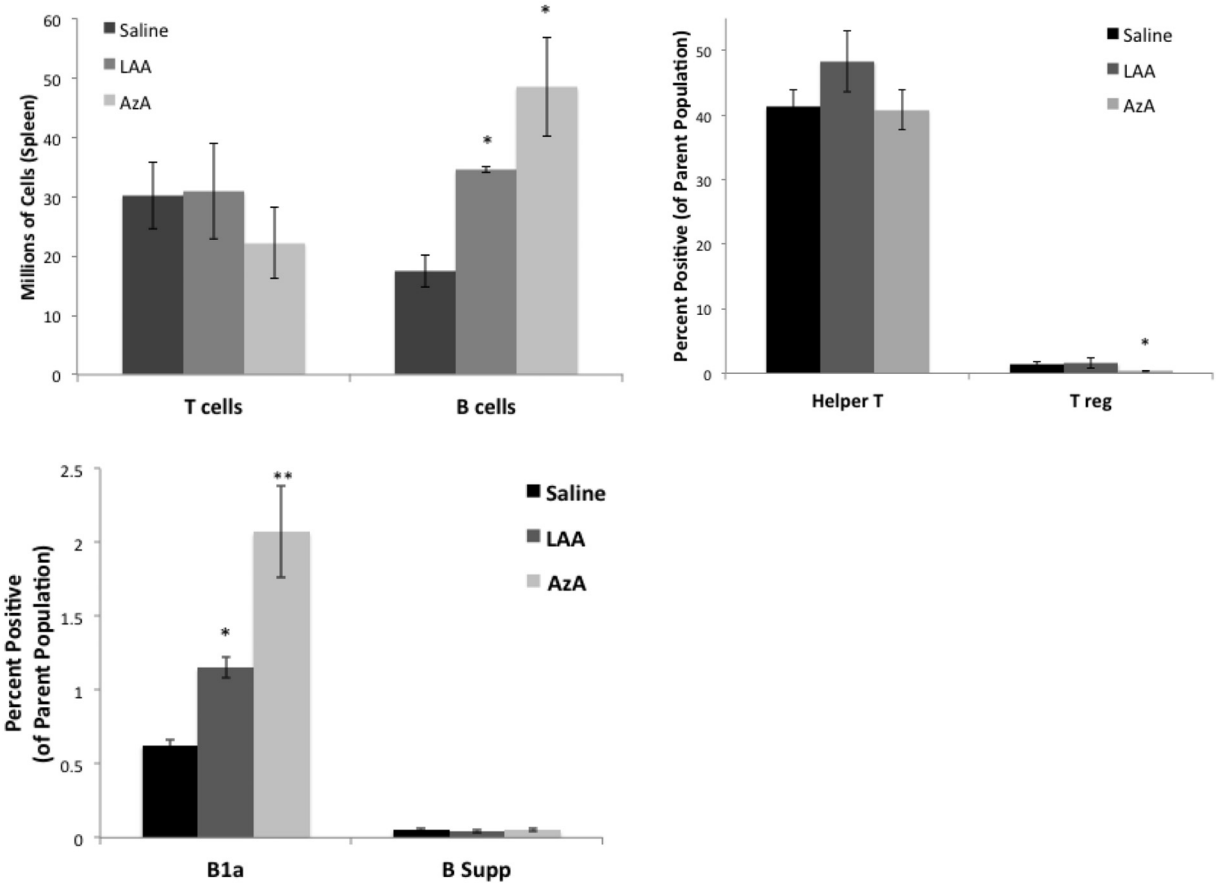

Fig. 6. Top left: T (CD3 +) and B (CD19 +) cells were identified in the lymphocyte gate by flow cytometry, using isotype controls to determine background values for positive staining. Percent positive was multiplied by the total number of lymphocytes. Top right: T cell subsets. CD3 + is parent for T helper; T helper is parent for Treg. Bottom: B cell subsets. Lymphocytes are parent for B1a; B1a is parent for B suppressors. Error bars = SEM. * = $p < 0.01$, ** = $p < 0.001$ compared to Saline control, by 2-tailed *t*-test and by one-way ANOVA.

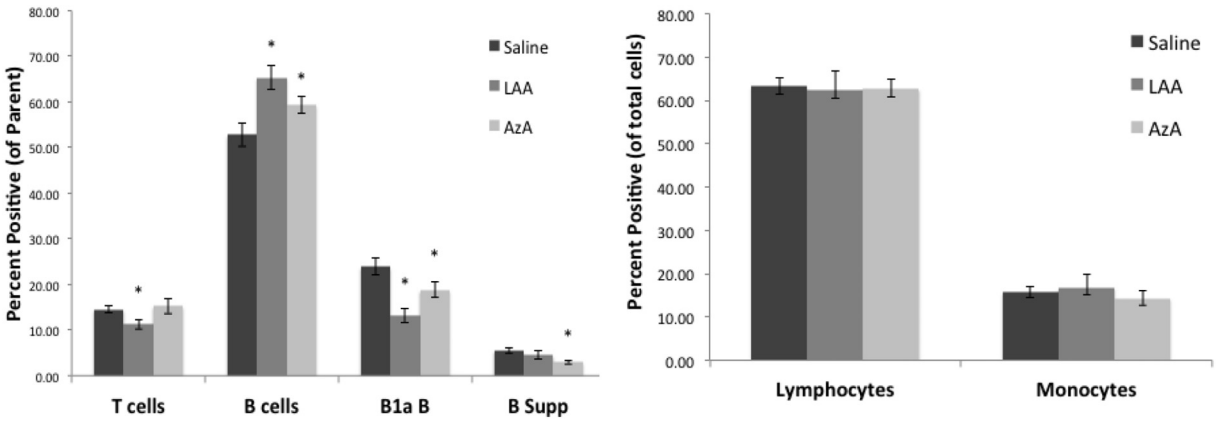

Fig. 7. Peritoneal Cell populations by flow cytometry. Top: Lymphocytes and monocytes were identified by Forward vs Side Scatter. Bottom: Lymphocyte subsets were identified by antibodies described in the Materials & Methods. Parent for T, B and B1a cells is Lymphocytes. Parent for B Supp are B1a B cells. Error bars = SEM. * = $p < 0.05$ compared to Saline controls.

(SAID) (Pfau et al., 2005; Noonan et al., 2006). The latter includes a rheumatic pain syndrome characterized by positive antinuclear autoantibody (ANA) tests, joint pain/swelling, and severe fatigue (Unpublished data, Libby Epidemiology Research Program). Mouse studies have supported these findings, such that the mouse model has proven to be extremely helpful in understanding some of these mechanisms. A key finding that was consistent in both mice and humans was that, while amphibole asbestos drives autoantibody production, chrysotile does not appear to do so, suggesting that immune effects could be fiber-specific (Ferro et al., 2013; Pfau et al., 2015). This may then affect down-stream disease manifestations and severity.

We undertook this study to test the hypothesis that what has been learned from LAA can be applied to novel "naturally occurring asbestos" (NOA). Such NOA is being discovered in many areas of the U.S. and around the world (Abakay et al., 2016; Bayram & Bakan, 2014; Buck et al., 2013; Metcalf & Buck, 2015), making it an emerging public health hazard. Due to the severity and latency of asbestos-related diseases, identification of exposures and early health risk assessment is essential in order to control/reduce exposure as much as possible.

This study is novel for two reasons. First, it includes a newly

Table 2
Peritoneal cell subpopulations by flow cytometry[a].

	Saline	LAA	AzAA	P value[b] (by treatments)
Monocytes				
Male	17.7 (4.5)	23.2 (9.8)[c]	18.2 (7.2)[c]	0.39
Female	12.2 (4.1)	11.7 (3.5)	11.3 (4.9)	0.93
Lymphocytes				
Male	63.1 (5.6)	55.4 (12.2)	60.5 (10.2)	0.37
Female	63.5 (10.6)	67.9 (11.7)	64.4 (6.7)	0.72
T cell				
Male	15.3 (3.4)	11.8 (4.4)	**21.4 (6.4)**[c]	0.01
Female	13.2 (3.1)	10.7 (1.6)	10.6 (2.5)	0.17
B cells				
Male	49.2 (9.4)	**63.2 (2.5)**	56.5 (7.6)	0.025
Female	59.3 (6.6)	66.9 (10.7)	61.6 (8.3)	0.37
B1a B cells				
Male	26.1 (7.1)	**12.5 (3.5)**	**18.1 (7.4)**	0.009
Female	19.9 (5.0)	13.6 (5.5)	19.3 (7.4)	0.23
B supp				
Male	4.9 (1.7)	6.0 (3.1)	4.1 (1.6)	0.34
Female	6.9 (3.2)	**3.3 (1.5)**[c]	**2.0 (1.2)**[c]	0.002

[a] Data shown as mean percent of parent population (std deviation).
[b] One Way ANOVA with post-hoc tests; **bold** = $p < 0.05$ compared to saline control.
[c] $p < 0.05$ compared to other sex.

Table 3
Serum cytokines by cytokine bead array[a].

	Saline	LAA	AzA	p value[b] treatment
IL-4	11.6 (0.37)	11.8 (0.32)	13.3 (2.2)	> 0.05
Male	11.5 (0.35)	11.9 (0.47)	12.6 (0.47)	> 0.05
Female	11.9 (0.15)	11.7 (0.15)	13.8 (3.0)	> 0.05
IL-10	69.0 (8.6)	**117.6 (54.5)**	**169.8 (30.6)**	< 0.01
Male	65.2 (8.0)	**163.6 (11.5)**	**185.3 (25.6)**	< 0.01
Female	76.0 (4.0)	80.8 (11.5)[c]	**156.1 (28.0)**	< 0.01
IL-2	7.0 (0.29)	6.9 (0.32)	6.7 (0.55)	> 0.05
Male	7.0 (0.27)	6.6 (0.53)	6.8 (0.39)	> 0.05
Female	7.1 (0.26)	7.3 (0.28)	6.6 (0.40)	> 0.05
IFN gamma	4.0 (0.77)	9.1 (5.2)	**10.9 (6.2)**	< 0.05
Male	3.8 (0.64)	**14.1 (2.4)**	**9.1 (1.9)**	< 0.05
Female	4.3 (0.96)	5.0 (0.98)[c]	12.5 (8.3)	> 0.05
TNF alpha	25.6 (2.2)	**41.6 (18.2)**	**64.2 (11.1)**	< 0.05
Male	25.1 (1.8)	**56.8 (18.0)**	**62.5 (8.8)**	< 0.05
Female	26.6 (2.7)	29.4 (2.4)[c]	**65.7 (13.2)**	< 0.05
IL-6	8.3 (1.1)	**10.5 (2.6)**	**20.2 (6.7)**	< 0.05
Male	7.9 (0.96)	**12.2 (3.1)**	**18.0 (1.0)**	< 0.05
Female	8.9 (1.1)	9.2 (1.1)	**22.1 (9.0)**	< 0.05
IL-17	1.4 (0.95)	**12.6 (2.5)**	**9.7 (3.1)**	< 0.01
Male	1.1 (0.88)	**10.8 (2.6)**	**8.6 (1.4)**	< 0.01
Female	1.9 (0.94)	**14.0 (1.4)**	**10.7 (3.9)**	< 0.01

[a] Data shown as mean concentration in pg/ml (std deviation).
[b] One Way ANOVA with post-hoc tests; **bold** = $p < 0.05$ compared to saline control.
[c] $p < 0.05$ compared to other sex.

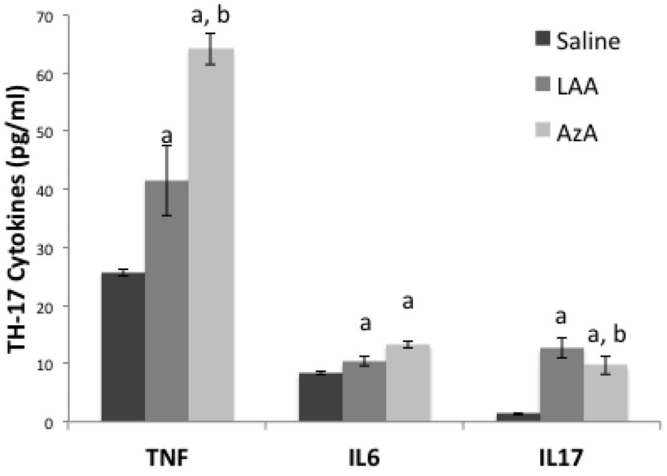

Fig. 8. Serum Cytokines by CBA. Cytokines of the T_H17 profile are shown. Error bars = SEM. a = $p < 0.01$ compared to Saline control, b = $p < 0.05$ compared to LAA.

Table 4
Male/female data comparison – spleen data.

	Saline	LAA	AzA
Spleen Weight, mg (SEM)			
Male	94.4 (6.4)	92.3 (2.5)	95.1 (4.8)
Female	98.8 (6.1)	116.0 (13.4)	128.7 (12.6)
Splenocytes/g mouse, millions (SEM)			
Male	1.55 (0.3)	2.36 (0.3)	1.08 (0.4)
Female	1.48 (0.1)	1.66 (0.2)	**3.26 (0.5)**[a,b]
Spleen B cells/g mouse, millions (SEM)			
Male	0.24 (0.04)	0.56 (0.2)	0.38 (0.1)
Female	0.19 (0.04)	0.33 (0.1)	**0.93 (0.2)**[a,b]
Spleen T cells/g mouse, millions (SEM)			
Male	0.39 (0.11)	0.47 (0.21)	0.35 (0.14)
Female	0.39 (0.04)	0.30 (0.05)	0.41 (0.09)
Spleen B cells, mean percent of lymphocytes (SEM)			
Male	43.4 (4.4)	58.0 (8.8)	**73.4 (2.5)**[b]
Female	31.5 (4.6)	52.7 (6.0)	**70.5 (4.6)**[b]
Spleen T cells, mean percent of lymphocytes (SEM)			
Male	56.7 (4.3)	42.0 (7.2)	**26.6 (2.5)**[b]
Female	68.5 (4.6)	47.3 (6.0)	**29.5 (4.6)**[b]

[a] 2-Tailed, unpaired *t*-test, **Bold**: $p < 0.05$ compared to other sex.
[b] One Way ANOVA with post-hoc tests; **Bold** = $p < 0.05$ compared to saline control.

described amphibole fiber mixture that has never been evaluated for health effects. Exposures to this material are occurring due to (a) widespread geographic occurrence of the fibrous amphiboles across southern Nevada and Arizona (Buck et al., 2013; Metcalf & Buck, 2015), (b) highly popular recreation sites in contaminated areas, creating large amounts of dust, (c) urban development expanding into and currently developed within the contaminated areas, and (d) the arid climate of this region that promotes naturally-generated asbestos-laden dust. Second, whereas we have used this mouse model to extensively study effects of LAA, we consistently used an exposure dose of 60–120 μg/mouse (Ferro et al., 2013; Pfau et al., 2008), closer to what could correspond to a high cumulative occupational exposure. The current study used only 3 μg/mouse, closer to what might occur as a periodic environmental exposure. Other fiber comparison studies provide some perspective on this dose: Gavett, et al., exposed rats to LAA in air at 0.5, 3.5, and 25 mg/m^3 for 6 h/day, 5 days/week for 13 weeks (Gavett et al., 2016). Taking into account rat respiratory rate and volume per day, and then calculating a total exposure per gram of rat, the total dose for the lowest exposure level was 3.74 μg/g of rat. This is comparable to our previous exposure dose of 60 μg/mouse (Ferro et al., 2013), calculated as 2.4 μg/g of mouse (considering a 25 g mouse). Another study used a mass dose per rat of 0.5 or 1.5 mg/rat, for which the lowest dose calculates to 1.2 μg/g of rat (Cyphert et al., 2012). Our current dose of 3 μg/mouse is 1/10th of even that low dose, calculating at 0.12 μg/g of mouse. It is therefore, to our knowledge, the lowest dose ever used in rodent models of asbestos exposure. The purpose for this, as mentioned above in the Methods, is that environmental exposures tend to be sporadic, due to dust storms or recreational activity in areas with naturally occurring asbestos, rather than regular, all day, work exposures. The cumulative exposure would thus be expected to be very low. The fact that significant effects were seen in the mice at the dose used in this study raises serious concern about such environmental

Table 5
Other male/female data comparisons.

	Saline	LAA	AzA
Urine albumin, % positive (# positive)			
Male	22.2 (2 of 9)	100 (4 of 4)	100 (7 of 7)
Female	0.0 (0 of 5)	75 (3 of 4)	63 (5 of 8)
Lung collagen, μg/mg lung (SEM)			
Male	1.2 (0.2)	**2.45 (0.05)**[b]	**2.4 (0.1)**[b]
Female	**2.1 (0.15)**[a]	2.3 (0.14)	2.4 (0.07)
Diaphragm collagen, μg/mg (SEM)			
Male	31.3 (7.1)	**67.7 (8.0)**[b]	**98.5 (17.9)**[b]
Female	27.5 (13.1)	**62.8 (20.7)**[b]	**65.6 (13.1)**[b]
MCAA, % positive (# positive)			
Male	11.1 (1 of 9)	25 (1 of 4)	50 (4 of 8)
Female	20 (1 of 5)	40 (2 of 5)	66 (6 of 9)
MCAA score, mean (SEM)			
Male	1.24 (0.79)	1.68 (1.32)	2.98 (0.81)
Female	1.76 (0.67)	1.74 (1.33)	4.88 (0.97)

[a] 2-Tailed, unpaired *t*-test, **Bold**: $p < 0.05$ compared to other sex.
[b] One Way ANOVA with post-hoc tests; **Bold** = $p < 0.05$ compared to saline control.

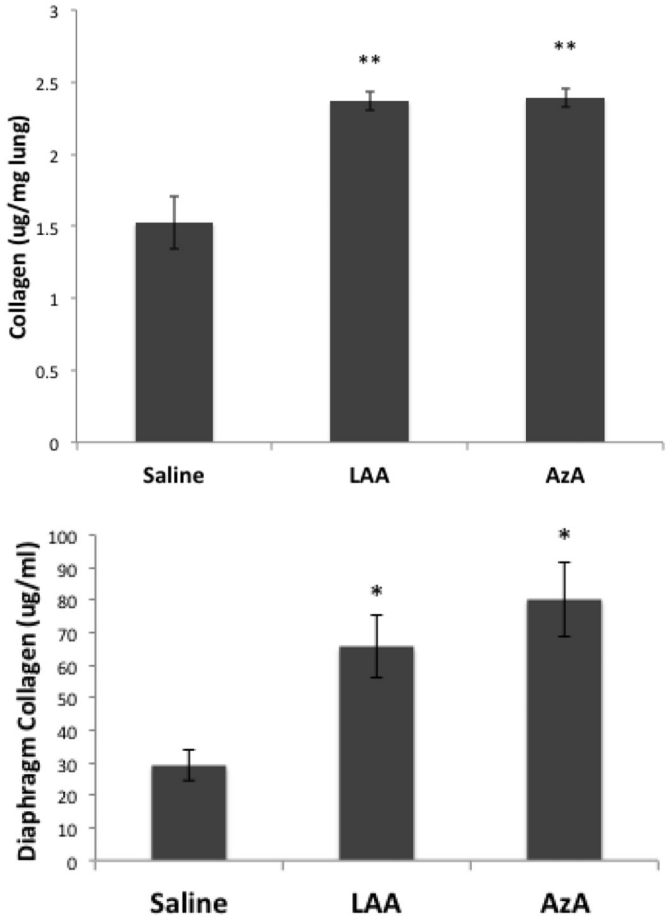

Fig. 9. Lung and Pleural Collagen by hydroxyproline assay (QuickZyme). Top: Total collagen in the right lung of each mouse was assayed and data are shown as μg of collagen per mg of wet lung tissue. ** = $p < 0.01$ compared to saline control. Bottom: Collagen in diaphragms (Parietal pleura). * = $p < 0.01$ compared to Saline.

exposures.

Using C57BL/6 mice, we compared the immune and pulmonary effects of this low level exposure to LAA and a mixture of fibrous amphibole asbestos from Arizona (AzA). The AzA is composed of winchite (76%) and actinolite (24%), which has very similar mineralogy to LAA, composed of winchite (83%), richterite (11%), and tremolite (9%) (Meeker et al., 2003) (Table 1). It is more difficult to compare particle morphology because different techniques were used to characterize the fibers (Table 1). The TEM analyses used for LAA allow for smaller particles to be imaged and analyzed as compared to the SEM analyses used for AzA. These differences likely explain much of the differences shown in Table 1 between AzA and LAA. However, overall, LAA has lower aspect ratios as compared to AzA both in the mean (8.4 ± 0.7 for LAA vs. 16.7 ± 0.9 for AzA whole sample including accessory minerals) as well as the percentage of particles with aspect ratios 3.0 or greater (49% for LAA; 86% for AzA).

4.1. Immune/inflammatory effects

In this study, AzA is at least as immunostimulatory as LAA. A higher dose LAA (60–120 μg/mouse) leads to 80% of mice having positive ANA tests (Ferro et al., 2013; Pfau et al., 2008; Zebedeo et al., 2014). However, at the current low dose, only AzA induced ANA above control frequencies. In the previous high dose studies, not only was the dose higher than what was used here, but only female mice were used (Ferro et al., 2013; Pfau et al., 2008). The current study shows that female mice are more likely to produce positive ANA tests; therefore, the inclusion of male mice in the current study affected the overall results. Another difference was that previous studies used intratracheal instillation, which likely affects both the size and quantity of fibers reaching the lower respiratory tract, compared to oropharyngeal aspiration used here, by bypassing the pharynx and upper trachea. A recent comparison of intratracheal, intranasal, and oropharyngeal aspiration of crystalline silica particles demonstrated comparable effects, but intratracheal instillation led to more dispersion of the particles throughout the lung and more potent inflammatory effects (Lacher et al., 2010). We used oropharyngeal aspiration in the current study to avoid surgical and pharmaceutical stressors, and to more closely model human exposures for these fibers. This method has been shown to be somewhat more effective at recapitulating outcomes seen in humans compared to intratracheal (Lacher et al., 2010; Egger et al., 2013; Lakatos et al., 2006).

Despite these differences, immune dysfunction was apparent in both male and female mice at the current low dose of both LAA and AzA, including a shift in lymphocyte subsets in both spleen and peritoneal cavity. In the spleen, the percentage of regulatory T cells was slightly reduced despite no overall difference in spleen weight, lymphocytes, or overall T cell numbers. This is consistent with our previous study showing reduced numbers of regulatory T cells in lymph nodes of amphibole-exposed mice (Pfau et al., 2008). Total spleen B cell numbers were increased with both LAA and AzA, and among those B cells, the proportion of B1a B cells was increased, again consistent with previous studies with LAA (Ferro et al., 2013; Pfau et al., 2013). B1a B cells have been implicated in autoantibody production and high numbers are seen in lupus-prone mouse strains (Duan & Morel, 2006; Mohan et al., 1998; Potula et al., 2012). Unlike our previous studies, there was no change in the frequency of splenic suppressor B cells with any treatment. However, AzA did cause a reduction in the frequency of both peritoneal B1a B cells and suppressor B cells, again consistent with previous studies for LAA (Ferro et al., 2013; Pfau et al., 2013). This suggests that activation and trafficking of B1a B cells to the spleen were affected. This is a key observation as the spleen is the site where these cells become active in producing autoantibodies (Pfau et al., 2013; Mohan et al., 1998).

Both LAA and AzA increased serum cytokines of the T_H17 response profile, but not T_H1 or T_H2 responses. This is consistent with our previous high doses studies with LAA as well (Ferro et al., 2013; Zebedeo et al., 2014). T_H17 responses have been implicated in autoimmune and inflammatory diseases (Afzali et al., 2007; Furuzawa-Carballeda et al., 2007; Kim et al., 2016). Both males and females contributed to the increases in T_H17 cytokines for both fibers.

4.2. Pulmonary effects

Both LAA and AzA induced interstitial and pleural fibrosis, which are well-known outcomes of asbestos exposure. In humans, the unique LPT of LAA is thought to occur primarily on the parietal pleura, but to also involve the visceral pleura (Szeinuk et al., 2016). There were no significant differences between LAA and AzA in terms of the quantity of collagen detected in lungs or diaphragms at this low dose. Untreated female mice had more lung collagen than males, and responded minimally to treatment. However, male mice had the significant increases in lung collagen with both fibers.

In humans and mice, there is an association between the presence of mesothelial cell autoantibodies (MCAA) and pleural fibrosis (Marchand et al., 2012; Gilmer et al., 2015). This is a critical finding due to the severe and progressive nature of the amphibole-induced LPT, since MCAA may prove to be a therapeutic target for slowing the progression or severity of disease (Gilmer et al., 2016; Hanson et al., 2016). Therefore, the induction of both MCAA and pleural fibrosis in this study, along with the ability of MCAA to induce serous fibrosis in mice in the absence of asbestos (Gilmer et al., 2015), provides evidence and justification for further study into the pathogenic role of MCAA.

4.3. Limitations and conclusions

The limitations of this study include the use of non-elutriated fibers and differences in fiber characterization methods. Elutriation is a method of collecting fibers, from a raw sample, that fall into a respirable range, meaning that the fibers would be expected to reach the small bronchioles and alveoli of the lung (Webber et al., 2008). Non-elutriated fibers were used in order to set the baseline in mouse studies where the full range of fiber sizes in collected samples was included (columns 1 and 3 in Table 1). Oropharyngeal exposures tend to leave larger particles and fiber bundles in the pharynx and upper airways, allowing the body to naturally sort a mixture of fibers into lung compartments. Additionally, the different techniques available to characterize fibers have their own limitations. Transmission electron microscopy (TEM/SAED) allows for analysis of smaller particles compared to SEM/EDS. Future studies using field-emission SEM may be able to better capture these smaller particles, and surface area analyses can also be used to better understand what characteristics might be driving the immune dysfunction.

In conclusion, these data support our hypothesis that other environmental fibrous amphiboles can have effects very much like LAA, even at very low doses in mice. This should raise the level of concern regarding exposures in southern Nevada, Arizona, and other places where natural processes and anthropogenic activities are generating dust.

Funding

This work was funded by a grant from the Montana Agricultural Experimental Station (MAES), Montana State University, Bozeman, MT.

Declarations of interest

The authors have no conflicts of interest to disclose.

Acknowledgements

We thank Isabella Aquino for assistance in collecting fiber characterization data.

References

Abakay, A., Tanrikulu, A.C., Ayhan, M., Imamoglu, M.S., Taylan, M., Kaplan, M.A., Abakay, O., 2016. High-risk mesothelioma relation to meteorological and geological condition and distance from naturally occurring asbestos. Environ. Health Prev. Med. 21 (2), 82–90.

Afzali, B., Lombardi, G., Lechler, R.I., Lord, G.M., 2007. The role of T helper 17 (Th17) and regulatory T cells (Treg) in human organ transplantation and autoimmune disease. Clin. Exp. Immunol. 148 (1), 32–46.

Antao, V.C., Larson, T.C., Horton, D.K., 2012. Libby vermiculite exposure and risk of developing asbestos-related lung and pleural diseases. Curr. Opin. Pulm. Med. 18 (2), 161–167.

Bandli, B.R., Gunter, M.E., 2006. A review of scientific literature examining the mining history, geology, mineralogy, and amphibole asbestos health effects of the Rainy Creek igneous complex, Libby, Montana, USA. Inhal. Toxicol. 18 (12), 949–962.

Baumann, F., Ambrosi, J.P., Carbone, M., 2013. Asbestos is not just asbestos: an unrecognised health hazard. Lancet Oncol. 14 (7), 576–578.

Baumann, F., Buck, B.J., Metcalf, R.V., McLaurin, B.T., Merkler, D.J., Carbone, M., 2015. The presence of asbestos in the natural environment is likely related to mesothelioma in young individuals and women from southern Nevada. J. Thorac. Oncol. 10 (5), 731–737.

Bayram, M., Bakan, N.D., 2014. Environmental exposure to asbestos: from geology to mesothelioma. Curr. Opin. Pulm. Med. 20 (3), 301–307.

Benson, R., Berry, D., Lockey, J., Brattin, W., Hilbert, T., LeMasters, G., 2015. Exposure-response modeling of non-cancer effects in humans exposed to Libby Amphibole Asbestos; update. Regul. Toxicol. Pharmacol. 73 (3), 780–789.

Black, B., Szeinuk, J., Whitehouse, A.C., Levin, S.M., Henschke, C.I., Yankelevitz, D.F., Flores, R.M., 2014. Rapid progression of pleural disease due to exposure to Libby amphibole: “not your grandfather's asbestos related disease”. Am. J. Ind. Med. 57 (11), 1197–1206.

Blake, D.J., Wetzel, S.A., Pfau, J.C., 2008. Autoantibodies from mice exposed to Libby amphibole asbestos bind SSA/Ro52-enriched apoptotic blebs of murine macrophages. Toxicology 246 (2–3), 172–179.

Buck, B.J., Goossens, D., Metcalf, R.V., McLaurin, B., Ren, M., Freudenberger, F., 2013. Naturally occurring asbestos: potential for human exposure, southern Nevada, USA. Soil Sci. Soc. Am. J. 77, 2192–2204.

Carbone, M., Kanodia, S., Chao, A., Miller, A., Wali, A., Weissman, D., Adjei, A., Baumann, F., Boffetta, P., Buck, B., de Perrot, M., Dogan, A.U., Gavett, S., Gualtieri, A., Hassan, R., Hesdorffer, M., Hirsch, F.R., Larson, D., Mao, W., Masten, S., Pass, H.I., Peto, J., Pira, E., Steele, I., Tsao, A., Woodard, G.A., Yang, H., Malik, S., 2016. Consensus report of the 2015 Weinman international conference on mesothelioma. J. Thorac. Oncol. 11 (8), 1246–1262.

Cooper, W.C., Murchio, J., Popendorf, W., Wenk, H.R., 1979. Chrysotile asbestos in a California recreational area. Science 206 (4419), 685–688.

Cyphert, J.M., Nyska, A., Mahoney, R.K., Schladweiler, M.C., Kodavanti, U.P., Gavett, S.H., 2012. Sumas Mountain chrysotile induces greater lung fibrosis in Fischer344 rats than Libby amphibole, El Dorado tremolite, and Ontario ferroactinolite. Toxicol. Sci. 130 (2), 405–415.

Duan, B., Morel, L., 2006. Role of B-1a cells in autoimmunity. Autoimmun. Rev. 5 (6), 403–408.

Duncan, K.E., Cook, P.M., Gavett, S.H., Dailey, L.A., Mahoney, R.K., Ghio, A.J., Roggli, V.L., Devlin, R.B., 2014. In vitro determinants of asbestos fiber toxicity: effect on the relative toxicity of Libby amphibole in primary human airway epithelial cells. Part Fibre Toxicol. 11, 2.

Dunning, K.K., Adjei, S., Levin, L., Rohs, A.M., Hilbert, T., Borton, E., Kapil, V., Rice, C., Lemasters, G.K., Lockey, J.E., 2012. Mesothelioma associated with commercial use of vermiculite containing Libby amphibole. J. Occup. Environ. Med. 54 (11), 1359–1363.

Egger, C., Cannet, C., Gerard, C., Jarman, E., Jarai, G., Feige, A., Suply, T., Micard, A., Dunbar, A., Tigani, B., Beckmann, N., 2013. Administration of bleomycin via the oropharyngeal aspiration route leads to sustained lung fibrosis in mice and rats as quantified by UTE-MRI and histology. PLoS One 8 (5), e63432.

Environmental Protection Agency, US, 2008. Clear Creek Management Area Asbestos Exposure And Human Health Risk Assessment, R. 9, Editor. U.S. EPA, San Franciso, CA.

Ferro, A., Zebedeo, C.N., Davis, C., Ng, K.W., Pfau, J.C., 2013. Amphibole, but not chrysotile, asbestos induces anti-nuclear autoantibodies and IL-17 in C57BL/6 mice. J. Immunotoxicol. http://dx.doi.org/10.3109/1547691X.2013.847510.

Furuzawa-Carballeda, J., Vargas-Rojas, M.I., Cabral, A.R., 2007. Autoimmune inflammation from the Th17 perspective. Autoimmun. Rev. 6 (3), 169–175.

Gavett, S.H., Parkinson, C.U., Willson, G.A., Wood, C.E., Jarabek, A.M., Roberts, K.C., Kodavanti, U.P., Dodd, D.E., 2016. Persistent effects of Libby amphibole and amosite asbestos following subchronic inhalation in rats. Part Fibre Toxicol. 13, 17.

Gilmer, J., Serve, K., Davis, C., Anthony, M., Hanson, R., Harding, T., Pfau, J.C., 2015. Libby amphibole induced mesothelial cell autoantibodies promote collagen deposition in mice. Am. J. Phys. Lung Cell. Mol. Phys. 2016 p. ajplung 00462.

Gilmer, J., Harding, T., Woods, L., Black, B., Flores, R., Pfau, J.C., 2016. Mesothelial cell autoantibodies upregulate transcription factors associated with fibrosis. Inhal. Toxicol (in press).

Hanson, R., Evilia, C., Gilmer, J., Woods, L., Black, B., Flores, R., Pfau, J.C., 2016. Libby amphibole-induced mesothelial cell autoantibodies bind to surface plasminogen and alter collagen matrix remodeling. Phys. Rep. 4 (7), 1–12.

Kim, B.S., Park, Y.J., Chung, Y., 2016. Targeting IL-17 in autoimmunity and inflammation. Arch. Pharm. Res. 39 (11), 1537–1547.

Lacher, S.E., Johnson, C., Jessop, F., Holian, A., Migliaccio, C.T., 2010. Murine pulmonary inflammation model: a comparative study of anesthesia and instillation methods. Inhal. Toxicol. 22 (1), 77–83.

Lakatos, H.F., Burgess, H.A., Thatcher, T.H., Redonnet, M.R., Hernady, E., Williams, J.P., Sime, P.J., 2006. Oropharyngeal aspiration of a silica suspension produces a superior model of silicosis in the mouse when compared to intratracheal instillation. Exp. Lung

Res. 32 (5), 181–199.
Larson, T.C., Meyer, C.A., Kapil, V., Gurney, J.W., Tarver, R.D., Black, C.B., Lockey, J.E., 2010a. Workers with Libby amphibole exposure: retrospective identification and progression of radiographic changes. Radiology 255 (3), 924–933.
Larson, T.C., Antao, V.C., Bove, F.J., 2010b. Vermiculite worker mortality: estimated effects of occupational exposure to Libby amphibole. J. Occup. Environ. Med. 52 (5), 555–560.
Larson, T.C., Antao, V.C., Bove, F.J., Cusack, C., 2012a. Association between cumulative fiber exposure and respiratory outcomes among Libby vermiculite workers. J. Occup. Environ. Med. 54 (1), 56–63.
Larson, T.C., Lewin, M., Gottschall, E.B., Antao, V.C., Kapil, V., Rose, C.S., 2012b. Associations between radiographic findings and spirometry in a community exposed to Libby amphibole. Occup. Environ. Med. 69 (5), 361–366.
Lockey, J.E., Dunning, K., Hilbert, T.J., Borton, E., Levin, L., Rice, C.H., McKay, R.T., Shipley, R., Meyer, C.A., Perme, C., LeMasters, G.K., 2015. HRCT/CT and associated spirometric effects of low Libby amphibole asbestos exposure. J. Occup. Environ. Med. 57 (1), 6–13.
Lowers, H.A., Wilson, S.A., Hoefen, T.M., Benzel, W.M., Meeker, G.P., 2012. Preparation and Characterization of "Libby Amphibole" Toxicological Testing Material, D.o.t. Interior, Editor. United States Geological Survey, Reston, VA, pp. 1–20.
Marchand, L.S., St-Hilaire, S., Putnam, E.A., Serve, K.M., Pfau, J.C., 2012. Mesothelial cell and anti-nuclear autoantibodies associated with pleural abnormalities in an asbestos exposed population of Libby MT. Toxicol. Lett. 208 (2), 168–173.
McDonald, J.C., Harris, J., Armstrong, B., 2004. Mortality in a cohort of vermiculite miners exposed to fibrous amphibole in Libby, Montana. Occup. Environ. Med. 61 (4), 363–366.
Meeker, G.P., Bern, A.M., Brownfield, I.K., Lowers, H.A., Sutley, S.J., Hoefen, T.M., Vance, J.S., 2003. The composition and morphology of amphiboles from the Rainy Creek complex, near Libby, Montana. Am. Mineraologist 88, 1955–1969.
Metcalf, R.V., Buck, B.J., 2015. Genesis and health risk implications of an unusual occurrence of fibrous NaFe3 + -amphibole. Geology 43 (1), 63–66.
Mohan, C., Morel, L., Yang, P., Wakeland, E.K., 1998. Accumulation of splenic B1a cells with potent antigen-presenting capability in NZM2410 lupus-prone mice. Arthritis Rheum. 41 (9), 1652–1662.
Noonan, C.W., 2006. Exposure matrix development for the Libby cohort. Inhal. Toxicol. 18 (12), 963–967.
Noonan, C.W., Pfau, J.C., Larson, T.C., Spence, M.R., 2006. Nested case-control study of autoimmune disease in an asbestos-exposed population. Environ. Health Perspect. 114 (8), 1243–1247.
Noonan, C.W., Conway, K., Landguth, E.L., McNew, T., Linker, L., Pfau, J., Black, B., Szeinuk, J., Flores, R., 2015. Multiple pathway asbestos exposure assessment for a superfund community. J. Expo. Sci. Environ. Epidemiol. 25 (1), 18–25.
Paoletti, L., Batisti, D., Bruno, C., Di Paola, M., Gianfagna, A., Mastrantonio, M., Nesti, M., Comba, P., 2000. Unusually high incidence of malignant pleural mesothelioma in a town of eastern Sicily: an epidemiological and environmental study. Arch. Environ. Health 55 (6), 392–398.
Peipins, L.A., Lewin, M., Campolucci, S., Lybarger, J.A., Miller, A., Middleton, D., Weis, C., Spence, M., Black, B., Kapil, V., 2003. Radiographic abnormalities and exposure to asbestos-contaminated vermiculite in the community of Libby, Montana, USA. Environ. Health Perspect. 111 (14), 1753–1759.
Pfau, J.C., Sentissi, J.J., Weller, G., Putnam, E.A., 2005. Assessment of autoimmune responses associated with asbestos exposure in Libby, Montana, USA. Environ. Health Perspect. 113 (1), 25–30.
Pfau, J.C., Sentissi, J.J., Li, S., Calderon-Garciduenas, L., Brown, J.M., Blake, D.J., 2008. Asbestos-induced autoimmunity in C57BL/6 mice. J. Immunotoxicol. 5 (2), 129–137.
Pfau, J.C., Hurley, K., Peterson, C., Coker, L., Fowers, C., Marcum, R., 2013. Activation and trafficking of peritoneal B1a B-cells in response to amphibole asbestos. J. Immunotoxicol (in press).
Pfau, J.C., Serve, K.M., Woods, L., Noonan, C.W., 2015. Asbestos Exposure and Autoimmunity, in Biological Effects of Fibrous and Particulate Substances. Springer Publications.
Potula, H.H., Xu, Z., Zeumer, L., Sang, A., Croker, B.P., Morel, L., 2012. Cyclin-dependent kinase inhibitor Cdkn2c deficiency promotes B1a cell expansion and autoimmunity in a mouse model of lupus. J. Immunol. 189 (6), 2931–2940.
Rohs, A.M., Lockey, J.E., Dunning, K.K., Shukla, R., Fan, H., Hilbert, T., Borton, E., Wiot, J., Meyer, C., Shipley, R.T., Lemasters, G.K., Kapil, V., 2008. Low-level fiber-induced radiographic changes caused by Libby vermiculite: a 25-year follow-up study. Am. J. Respir. Crit. Care Med. 177 (6), 630–637.
Serve, K.M., Black, B., Szeinuk, J., Pfau, J.C., 2013. Asbestos-associated mesothelial cell autoantibodies promote collagen deposition in vitro. Inhal. Toxicol. 25 (14), 774–784.
Sullivan, P.A., 2007. Vermiculite, respiratory disease, and asbestos exposure in Libby, Montana: update of a cohort mortality study. Environ. Health Perspect. 115 (4), 579–585.
Szeinuk, J., Noonan, C.W., Henschke, C.I., Pfau, J., Black, B., Miller, A., Yankelevitz, D.F., Liang, M., Liu, Y., Yip, R., Linker, L., McNew, T., Flores, R.M., 2016. Pulmonary abnormalities as a result of exposure to Libby amphibole during childhood and adolescence-the pre-adult latency study (PALS). Am. J. Ind. Med.
Tetra Tech, I, 2014. Phase I Site Characterization Report for Boulder City Bypass Naturally Occurring Asbestos (NOA) Project: Railroad Pass to Silverline Road. Nevada Department of Transportation, Helena MT, pp. 1–118.
U.S. Environmental Protection Agency, R, 2011. Libby Asbestos Superfund Site Operable Unit 3 Initial Screening Level Human Health Risk Assessment for Exposure to Asbestos. US EPA.
U.S. Environmental Protection Agency, R, 2015. Site-wide Human Health Risk Assessment - Executive Summary - Libby Asbestos Superfund Site, Libby, Montana, R. 8, Editor. CDM Smith.
Van Gosen, B.S., 2007. The geology of asbestos in the United States and its practical applications. Environ. Eng. Geosci. 13 (1), 55–68.
Webber, J.S., Blake, D.J., Ward, T.J., Pfau, J.C., 2008. Separation and characterization of respirable amphibole fibers from Libby, Montana. Inhal. Toxicol. 20 (8), 733–740.
Whitehouse, A.C., 2004. Asbestos-related pleural disease due to tremolite associated with progressive loss of lung function: serial observations in 123 miners, family members, and residents of Libby, Montana. Am. J. Ind. Med. 46 (3), 219–225.
Whitehouse, A.C., Black, C.B., Heppe, M.S., Ruckdeschel, J., Levin, S.M., 2008. Environmental exposure to Libby asbestos and mesotheliomas. Am. J. Ind. Med. 51 (11), 877–880.
Winters, C.A., Hill, W.G., Rowse, K., Black, B., Kuntz, S.W., Weinert, C., 2012. Descriptive analysis of the respiratory health status of persons exposed to Libby amphibole asbestos. BMJ Open 2 (6).
Wylie, A.G., Candela, P.A., 2015. Methodologies for determining the sources, characteristics, distribution, and abundance of asbestiform and nonasbestiform amphibole and serpentine in ambient air and water. J. Toxicol. Environ. Health B Crit. Rev. 18 (1), 1–42.
Zebedeo, C.N., Davis, C., Pena, C., Ng, K.W., Pfau, J.C., 2014. Erionite induces production of autoantibodies and IL-17 in C57BL/6 mice. Toxicol. Appl. Pharmacol. 275 (3), 257–264.